ISSN 2075-1133, Inorganic Materials: Applied Research, 2020, Vol. 11, No. 5, pp. 1093–1102. © Pleiades Publishing, Ltd., 2020.
Russian Text © The Author(s), 2020, published in Perspektivnye Materialy, 2020, No. 5, pp. 23–37.

MATERIALS OF POWER ENGINEERING AND RADIATION-RESISTANT MATERIALS

Damage and Deformation Effects in the Surface Layers of Copper and Copper–Gallium Alloy under Pulsed Irradiation in a Plasma Focus Unit

I. V. Borovitskaya[a, *], V. A. Gribkov[a, **], A. S. Demin[a, *], N. A. Yepifanov[a, b, ****], S. V. Latyshev[a, c, *****], S. A. Maslyaev[a, ******], Ye. V. Morozov[a, *******], V. N. Pimenov[a, ********], I. P. Sasinovskaya[a, *********], G. G. Bondarenko[b, **********], A. I. Gaidar[d, ***********], and M. Scholz[e]**

[a] *Baikov Institute of Metallurgy and Materials Science, Russian Academy of Sciences, Moscow, 119334 Russia*
[b] *National Research University Higher School of Economics, Moscow, 101000 Russia*
[c] *Moscow Technical University of Communications and Informatics, Moscow, 111024 Russia*
[d] *Research Institute of Advanced Materials and Technologies, Moscow, 115054 Russia*
[e] *Institute of Nuclear Physics, Krakow, 31-342 Poland*

**e-mail: symp@imet.ac.ru*
***e-mail: gribkovv@rambler.ru*
****e-mail: casha@bk.ru*
*****e-mail: mophix94@gmail.com*
******e-mail: latyshevsv@rambler.ru*
*******e-mail: maslyaev@mail.ru*
********e-mail: lieutenant@list.ru*
*********e-mail: pimval@mail.ru*
**********e-mail: porfirievna@mail.ru*
***********e-mail: gbondarenko@hse.ru*
************e-mail: niipmt@mail.ru*

Received January 14, 2020; revised February 18, 2020; accepted February 20, 2020

Abstract—The results of experiments concerning the irradiation of copper and Cu-10% Ga alloys by pulsed fluxes of deuterium plasma (DP) and deuterium ions (DI) performed using a Plasma Focus (PF) unit are presented. The technique of investigation is described. Damage and deformation effects in the surface layers of the mentioned materials after the irradiation of each material in two modes are studied. In one case, the irradiation is performed by a pulsed deuterium plasma at a power density of $q_{pl} = 10^7$ W/cm^2 and at pulse duration of $\tau_{pl} = 100$ ns. In another case, the pulsed fluxes of deuterium ions at $q_i = 10^8$–10^{11} W/cm^2, $\tau_i = 50$ ns act simultaneously with a dense deuterium plasma at $q_{pl} = 10^8$–10^9 W/cm^2, $\tau_{pl} = 100$ ns. Under a less severe irradiation mode (only plasma flux), the levels of damage in the case of both materials are close to each other. In the melted surface layer (SL), there are an undulated surface, craters, and micropores. Under the influence of thermal stresses, a plastic deformation is observed in the SL of the alloy, whereas in the case of pure copper this process is not observed under this irradiation mode. Damage to both materials in a more severe irradiation mode with the pulsed fluxes of deuterium ions and deuterium plasma is enhanced and accompanied by the SL erosion and sometimes by a deposition of microparticles of elements contained in the functional materials of the PF chamber onto the irradiated surface. The most significant damage is observed in the SL of Cu–10% Ga alloy, which, along with the action of powerful plasma beam fluxes, experiences a shock-wave impact. In this irradiation mode, plastic deformation is observed in the SL of each of the materials under consideration. In the case of pure copper (at $q = 10^8$–10^9 W/cm^2), the plastic deformation is observed in separate local microvolumes of SL, whereas in the case of copper-gallium alloy at $q = 10^{10}$–10^{11} W/cm^2 this process occurs within the entire irradiated SL. In this case, plastic deformation occurs both under the action of shock-wave mechanical loads and under the action of thermal stresses.

Keywords: pulsed fluxes, deuterium plasma, deuterium ions, plasma focus, damage, copper-gallium alloy, plastic deformation

DOI: 10.1134/S2075113320050056

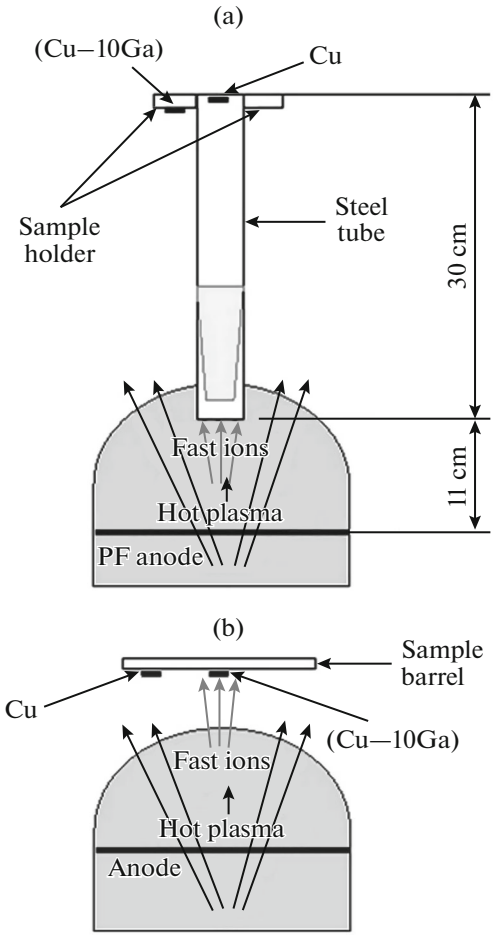

Fig. 1. Schematic diagram for the irradiation of samples made of pure Cu and Cu–10% Ga alloy using the PF-1000 unit with different sample holders: (a) hexagonal tube, (b) barrel.

INTRODUCTION

It is known that copper and copper-based alloys, mainly brass and bronze, have a number of properties useful for practical use such as high plasticity, electrical and thermal conductivity, corrosion resistance, and sufficient strength. Owing to this, copper and its alloys are widely used in different industries such as electrical engineering, radio electronics, instrument making, the chemical industry, mechanical engineering, and other fields of engineering.

Currently, in order to study the mechanisms that promote the improvement of the mechanical and technological properties of copper and copper alloys, studies concerning the influence of different external factors upon the structural state of these materials are performed. An important place is occupied by the development of such treatment methods that generate high-speed deformation processes in the materials leading to a change in the structural and phase state and the development of crystalline structures having new properties.

Among such methods, one should distinguish dynamic channel-angular pressing [1] based on the use of high-energy pulsed sources—the products of gunpowder explosion or combustion, exposure of the material to powerful ion beams [2, 3], pulsed laser radiation [4], and shock waves [5]. Thus, the authors of [5] considered effects caused by uniform and localized deformation, as well as dispersed structures formed in copper in copper alloys based on the Cu–Zn and Cu–Al systems using the following three methods of pulsed action. They are represented by converging shock waves, explosion-accelerated powder particles, and dynamic high-speed pressing.

Copper and copper-based Cu–10% Ga alloy were chosen for investigation in this work as model plastic materials resistant to cracking and to possible fracture under pulsed shock loads typical of thermonuclear plants with the inertial plasma confinement.

This work was aimed at comparing the features of damage and deformation effects in the surface layers of copper and copper-gallium alloy caused by the action of powerful pulsed fluxes of deuterium plasma and fast deuterium ions, as well as shock waves occurring in the materials in severe irradiation modes.

EXPERIMENTAL

The schematic of irradiation of samples in the Plasma Focus (PF) unit is shown in Fig. 1. Samples made of M1 grade copper (99.95% Cu, 0.05% O_2) and Cu–10% Ga alloy (hereinafter wt %), smelted using a vacuum furnace and representing a solid solution of gallium in copper, were used as the materials under study. The irradiated samples were in the form of tablets with a diameter of 9 mm and a thickness of 2 mm. All the experiments were performed using a PF-1000 unit with energy storage amounting to 600 kJ. As the working gas in the irradiation experiments, we used deuterium at chamber pressure $P = 470$ Pa.

Each of the samples was irradiated under two different conditions such that in one case the samples could experience a combined effect exerted by the pulsed fluxes of deuterium ions (DI) and those of dense deuterium plasma (DP), whereas in the other case the samples experienced only the effect of pulsed DP. For this, we used the two modes of irradiation (see Figs. 1a and 1b). In mode I, the samples of copper and Cu–10% Ga alloy were fixed on the rear end of a hexagonal tube made of 10Cr12Mn20W grade steel (Fig. 1a), whereas in mode II, the samples were placed on the wall of the barrel holder made of Cr18Ni9Ti steel facing the plasma beam flux and spaced at a distance of 12 cm from the anode (Fig. 1b).

In both cases, the target samples were located in the cathode zone of the PF chamber. Both samples (copper and alloy) fixed on the steel tube were located at the maximum distance from the anode of the PF unit and could mainly experience the only the effect of

Table 1. The irradiation parameters for the samples of Cu and Cu–10% Ga alloy in the PF-1000 unit

Sample	Distance from anode, L, cm	Power density DP, q_{pl}, W/cm^2	Pulse durationDP, τ_{pl}, ns	Power density ID, q_i, W/cm^2	Pulse duration ID, τ_i, ns	Number of acting pulses, N
Experiment 1						
Cu	41	10^7	100	–	–	
Cu–10% Ga	40	10^7	100	—	—	4
Experiment 2						
Cu	12	10^8–10^9	100	10^9–10^{10}	50	5
Cu–10% Ga	12	10^9	100	10^{11}	50	5

DP fluxes. The Cu–10% Ga alloy located outside the tube (Fig. 1a) was almost completely shielded by the tube wall from the action of DI fluxes and could be irradiated only by the DP propagating from the anode along the outer surface of this wall. The copper sample fixed on the axis of the tube in the center of its rear end was shielded also from the action of DI fluxes owing to the difference in the mechanisms of plasma flux and fast charged ion beam transport inside the tube.

As shown in [6, 7], owing to a higher velocity of fast high-energy ions ($u_i \sim 3 \times 10^8$ cm/s) in comparison with the velocity of the front boundary of the plasma cloud ($u_{pl} \sim (3–5) \times 10^7$ cm/s), at the stage of advancing the front of the plasma flux inside the tube by the high-energy ions, an effect of positively charged ion beam scattering on the inner surface of the tube in a certain zone of the tube is observed. This effect is accompanied by an intense ion bombardment of this surface, as well as by the most severe damage thereof in this area.

The estimates and the performed experiments [6–8] have shown that the effect under consideration is exerted at a distance of about 2/3 of the length of this tube from its front end, whereas the dominant energy flux, acting in this case on the Cu sample, is also represented by the plasma flux. The action of atoms and ions on the copper target could be, to all appearances, associated with the evaporation of elements from the surface of the sample holder made of steel, as well as from the inner wall of the tube in the course of the intense bombardment by deuterium ions at the moment of the beam scattering, with a subsequent deposition of the evaporated elements onto copper.

The samples of Cu and Cu–10% Ga alloy fixed on a barrel holder (Fig. 1b) were affected by both fluxes, DI and DP, but the copper-gallium alloy, located on the axis of the working chamber normally to the incident energy flux, experienced a more intense energy impact in comparison with the Cu sample placed on the barrel periphery. If the plasma flux acts on each of the samples to approximately the same extent, then the ion beam with ion energy $E_i > 100$ keV exerts a greater effect on the alloy.

This could be connected with the fact that the solid angle of divergence for the most powerful component of the ion beam does not exceed approximately 7°–10°, whereas the angle of the scattering cone of the total number of fast ions generated in the PF unit ranges within 20°–30° [7]. Therefore, the copper sample displaced from the chamber axis by ~3 cm (Fig. 1b) was exposed to the irradiation by a not so powerful component of the ion beam because it fell on the irradiated surface at an angle of ~15°, rather than normally.

The irradiation parameters for the samples are presented in Table 1, wherein experiments with the use of a hexagonal tube are called Experiment 1, and experiments with the use of a holding barrel are called Experiment 2.

After the irradiation, the samples were examined by means of optical microscopy (OM) and scanning electron microscopy (SEM) using a Neophot microscope and an EVO 40 scanning electron microscope (Zeiss) equipped with an attachment for local X-ray spectral analysis (XSA), respectively. The evolution of temperature in the irradiated surface layers, as well as the formation and propagation of shock waves under severe irradiation modes of target samples, was estimated by means of numerical simulation using approaches described in [9, 10].

RESULTS AND DISCUSSION

Irradiation of Copper Samples

Figure 2 shows the microstructure of copper samples after irradiation under the conditions of Experiment 1 and Experiment 2. It can be seen that in both cases the irradiation of the material led to the melting of the SL with the formation, after its solidification, of an undulating surface relief and typical structural defects such as drop-shaped fragments, micropores, sagging, and craters after the solidification of the molten surface.

In Experiment 1, the copper target was irradiated only with the fluxes of relatively diffused plasma, whereas in Experiment 2, the target was jointly

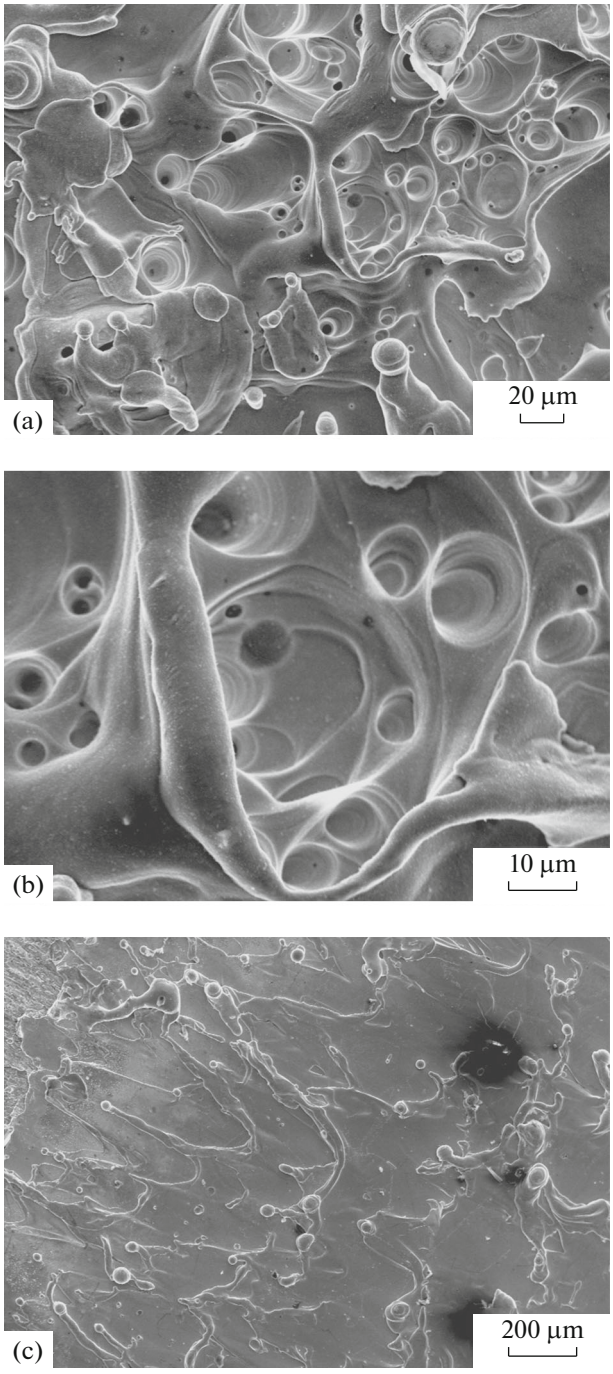

Fig. 2. SEM image of surface microstructure for pure copper samples after irradiation using the PF unit: (a, b) Experiment 1, (c) Experiment 2.

affected by more powerful fluxes of plasma and by the fluxes of fast deuterium ions (Fig. 1b, Table 1). The latter, in addition to the melting in the SL, led to surface erosion (the mass removal under evaporation).

A significant weight loss observed in Experiment 2 at each pulsed action of energy fluxes on Cu influenced the character of damage to the SL and the morphology of the irradiated surface. This can be clearly seen from the comparison of the microstructure in the cases under consideration (Figs. 2a, 2b compared to Fig. 2c). The concentration of structural fragments (droplets, craters, bulges, micropores) that occur on the Cu surface under a weaker radiation action in Experiment 1 is noticeably higher than that under more powerful energy fluxes observed in Experiment 2.

This, at first glance, paradoxical result is determined by the action of the pressure of secondary plasma formed in Experiment 2 in front of the surface facing the radiation flux in the course of pulsed discharges owing to the erosion process. The pressure effect exerted by the secondary plasma on the molten SL promotes a change in the surface morphology and a smoothing of the surface relief [8, 10]. In the case of very weak erosion or in the absence thereof (in Experiment 1), the number of structural inhomogeneities such as droplets, bulges, and craters occurring in the irradiated SL under several impulsive actions N, as a rule, exhibits an increase with increasing N and tends to a certain limit.

At the same time, owing to a strong erosion that is enhanced under the action of ion beams (with the target sample approaching the PF anode), an evaporation-driven removal at each pulsed action of some structural fragments present on the surface of the target sample occurs and thereby promotes a decrease in the total density thereof (Fig. 2c) and the formation of secondary plasma.

The analysis of copper samples based on optical microscopy has made it possible to reveal some signs of plastic deformation such as lines resembling slip traces or shear bands [11] within some local microvolumes of the target sample SL irradiated under more severe conditions using the barrel holder in Experiment 2 (Fig. 3). In these local zones, the deformation process occurs under the influence of thermal stresses arising in the SL at the stage of cooling after solidification of the liquid phase, as well as after the action of SW generated in the bulk of the material owing to powerful pulsed ion fluxes [10].

The effect of thermal stresses was determined by relatively long-term processes of melt solidification and subsequent SL cooling, whereas the action of SW has a pulsed character. It can be assumed that both of these factors exert a different effect on the mechanism of plastic deformation that occurs in the local zones of the irradiated SL of copper.

The X-ray spectral analysis of copper samples has shown that there is a lot of sulfur on the surface of the sample irradiated in Experiment 2 (Fig. 4).

Sulfur is present as an impurity in each of the steels from which the sample holders and the hexagonal tube were made [12]. The presence of sulfur on the surface of irradiated copper samples is most likely associated with evaporation of sulfur in the course of pulsed discharges from the surface of sulfur-containing func-

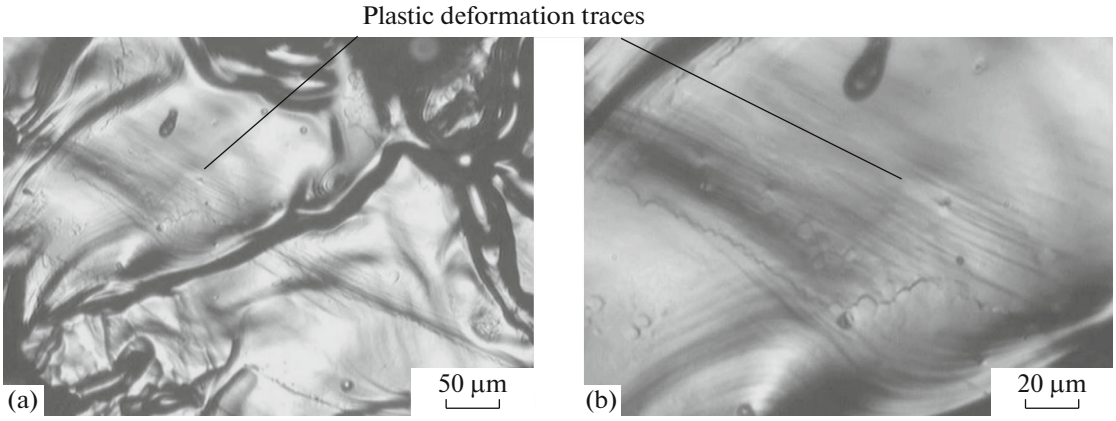

Fig. 3. OM images of the surface microstructure for a Cu sample irradiated with deuterium plasma and deuterium ions in Experiment 2.

tional materials located in the PF chamber, rather than from the steel tube and steel sample holders. This is indicated by the absence of traces of other elements from these steels in the irradiated SL of copper.

A typical character of sulfur distribution throughout the area of the irradiated surface of Cu sample is shown in Fig. 5.

Bright light points in Fig. 5 correspond to local areas with a high sulfur content. Since sulfur is almost insoluble in solid copper [13], it is accumulated mainly in the zones of discontinuities such as voids and grain boundaries and can also be involved in separate particles on the surface of the copper target (point *3* in Fig. 5).

Irradiation of Cu–10% Ga Alloy

Figure 6 shows a SEM image for the microstructure of the irradiated areas on the surface of Cu–10% Ga alloy after Experiment 1 using a hexagonal tube.

In Fig. 6, one can see structural fragments characteristic of a fused SL that occurred in the course of irradiation such as micropores, craters, and an undulating surface that in comparison with the irradiated sample of pure copper has a smoother relief. In addition, a blocklike character of the microstructure is observed, which reflects the fact that the process of plastic deformation in the material proceeds in the SL of the alloy under the conditions of radiation-thermal effects.

Twinning is one of the possible mechanisms of this process. This mechanism is facilitated by a decrease in stacking fault energy E_{pd}, which in the case of copper-based alloys (including the Cu–10% Ga alloy) is, as a rule, lower than that for pure copper [11]. The comparison of samples irradiated under the same conditions in Experiment 1 (Table 1) makes it possible to conclude that, in the solid solution of gallium in copper under the conditions of plasma beam action, a critical value of the reduced shear stress under which twins should be formed has been attained. For the alloys based on Cu, this value is in the range of σ_{cr} = 0.4–1.2 MPa [14]. From Fig. 6, it follows that the thermal stresses occurring in the SL of the Cu–10% Ga alloy at the stage of ultrafast crystallization of the liquid phase exceed the value of σ_{cr}, which facilitates the process of plastic deformation in the irradiated SL.

The irradiation of less plastic materials (W, Mo, V, etc.) under the conditions close to those considered above often leads to a cracking of the SL [15–19].

The boundaries forming the blocks on the irradiated alloy surface (Fig. 6) are decorated with carbon (Fig. 7). Carbon could have been deposited on the surface of the alloy from the gas phase, wherein it was contained as an impurity element and accumulated in the SL in the zone of an increased concentration of defects, i.e., at the boundaries of the blocks.

Figures 8 and 9 show OM and SEM images for the microstructure of the surface areas observed on the

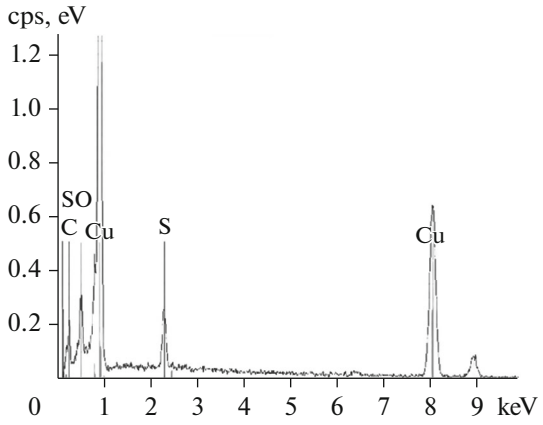

Fig. 4. The elemental composition copper surface after exposure to deuterium plasma in Experiment 2.

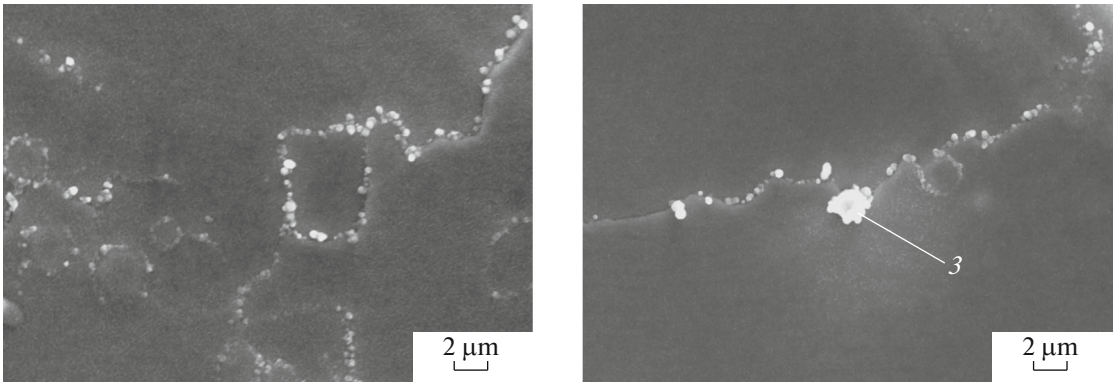

Fig. 5. SEM image of sulfur distribution on the surface of different areas of Cu sample fixed in a barrel holder (Experiment 2) after pulsed exposure to the fluxes of deuterium plasma and deuterium ions.

Cu–10% Ga alloy irradiated in Experiment 2 (Fig. 1b, Table 1).

The analysis has shown that, under the severe irradiation mode, more significant damage to the alloy surface is observed in comparison with the irradiation in Experiment 1 (Fig. 6), associated with a sweating and erosion of the SL, as well as with the evaporation and redeposition of the elements of functional materials (from the sample holder and PF anode) onto the alloy.

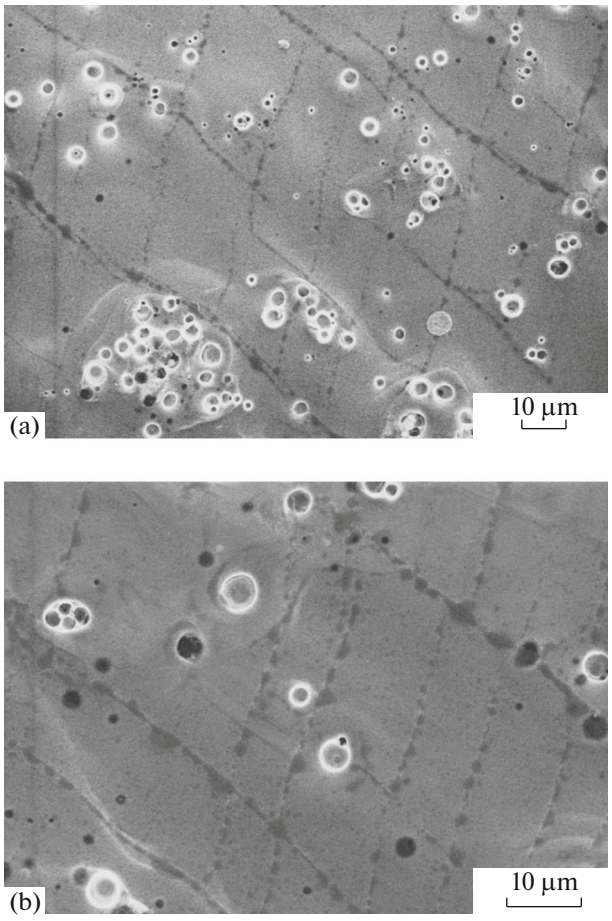

Fig. 6. SEM images of the surface microstructure of the Cu–10% Ga alloy at different magnifications after exposure to deuterium plasma flux with the use of the PF unit in Experiment 1.

Along with the undulating relief, micropores, and craters, the surface of the Cu–10% Ga alloy contains microparticles with a size of ~0.5–2 μm, as well as bubbles, some of which have destroyed dome-like lids (Fig. 8b). In addition, the blocky character of the surface microstructure (Fig. 9) indicates that a plastic deformation process occurs in the irradiated SL.

The results of X-ray spectral analysis presented in Fig. 10 has shown that the irradiated SL of the Cu–10% Ga sample in addition to the initial Cu and Ga contains such elements as Fe, C, and S. These elements are contained both in the alloy and in the microparticles deposited onto the alloy surface. In addition, Cu is present in many microparticles (Fig. 10a, point *4*). These microparticles, which, as a rule, have the form of droplets, were deposited on the surface of the alloy after the evaporation of the material from the PF anode according to the cluster mechanism under the action of a powerful electron beam inherent in pulsed discharges. Such elements as Fe, C, and S were involved in the composition of the steel barrel holder, and after the evaporation from the holder surface by DP and DI fluxes, they were partially deposited onto the surface of the irradiated alloy.

The bubbles observed in the SL of the alloy after the irradiation (Figs. 8, 9b) could have arisen owing to the evaporation of implanted deuterium ions from the zones of their capture by micropores and vacancy complexes, as well as owing to the formation of a vapor phase in the course of interaction between deuterium ions and the impurity oxygen present in the alloy.

This higher damageability of the Cu–10% Ga alloy in the considered severe irradiation mode is determined not only by the more intense radiation-thermal effect of the DI and DP fluxes but also by the action of acoustic and shock waves.

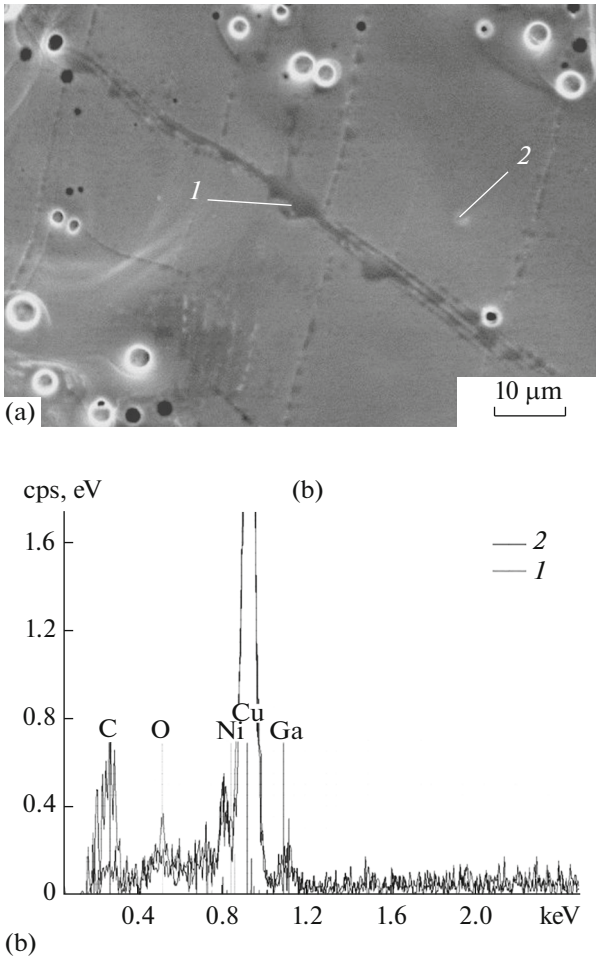

Fig. 7. (a) SEM image of the surface microstructure of the Cu–10 Ga alloy after the action of deuterium plasma in Experiment 1; (b) X-ray spectrum of elements at two points—at the interface between the blocks (point *1*) and near the interface (point *2*).

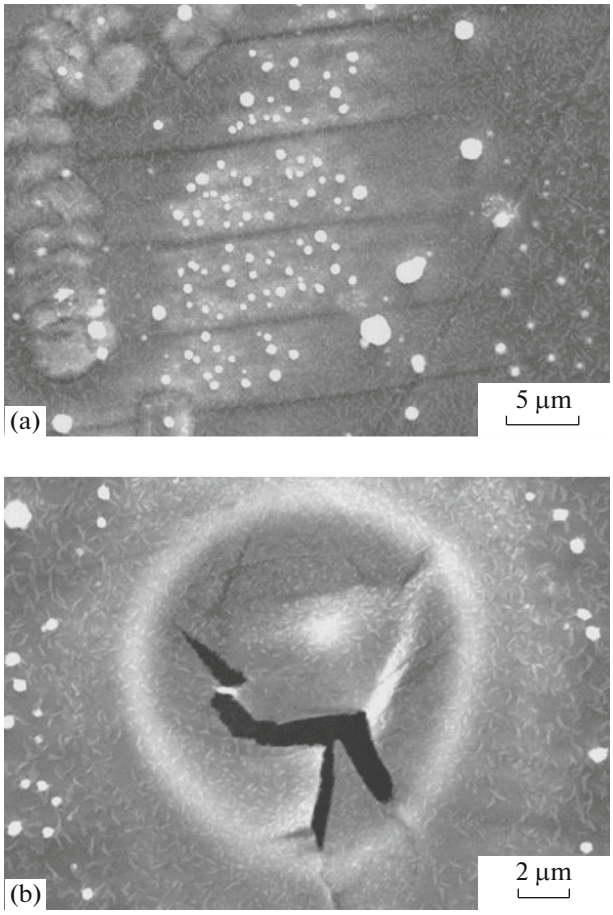

Fig. 8. SEM image of the surface microstructure of the Cu–10% Ga alloy at different magnifications after the action of deuterium plasma and deuterium ions in the PF unit (Experiment 2).

Table 2 shows the results of numerical evaluation [8, 10] for the thickness of the molten and evaporated layers of copper-gallium alloy for a single pulsed discharge in the PF unit, as well as for the SW pressure amplitude. The shock wave appears in the alloy under a severe irradiation mode at the end of the ion beam action as a recoil reaction with respect to the explosive evaporation of the material from the surface [3, 4, 8]. For the calculations, we have taken the density of the ion energy flux $q_i = 10^9$—2×10^{11} W/cm^2; the shape of the ion beam pulse being a half-sinusoid, $q(t) = q_0 \sin(\pi t/\tau)$ with a base duration of $\tau = 100$ ns; and the range of deuterium ions with the energy of $E_i = 100$ keV in the alloy $d = 1$ μm.

According to the accepted approximation, from Table 2, it follows that, upon a single-pulsed plasma beam action on the Cu–10% Ga alloy, a considerable erosion of the alloy SL occurs. So, for $q_i = 10^9$ W/cm^2, a layer with a thickness of ~0.3 μm is evaporated, whereas a layer with a thickness of ~10 μm is melted, and near the irradiated surface a shock wave is formed having a frontal pressure of ~0.4 GPa. For $q_i = 2 \times 10^{11}$ W/cm^2, the corresponding parameters are as follows: L_{evap} ~ 11 μm, L_{molt} ~ 30 μm, P_{SW} ~ 20 GPa.

Table 2. The thickness of the molten and evaporated layers and the amplitude of shock-wave pressure in the Cu–10% Ga alloy under pulsed discharge

q, W/cm^2	τ, ns	T, eV	L_{evap}, μm	L_{molt}, μm	P_{SW}, GPa
2×10^{11}	100	35	11	30	20
10^{10}	100	20	1.4	25	2.7
10^9	100	10	0.3	10	0.4

q is the maximum intensity of the ion beam, τ is the duration of the ion beam at the half-sinusoid base, T is the temperature of the secondary plasma originating from the target at the moment of the maximum intensity of the ion beam, L_{evap} and L_{molt} are the thickness of the evaporated and molten layers of the target sample, and P_{SW} is the pressure amplitude of the shock wave at the end of the ion beam action.

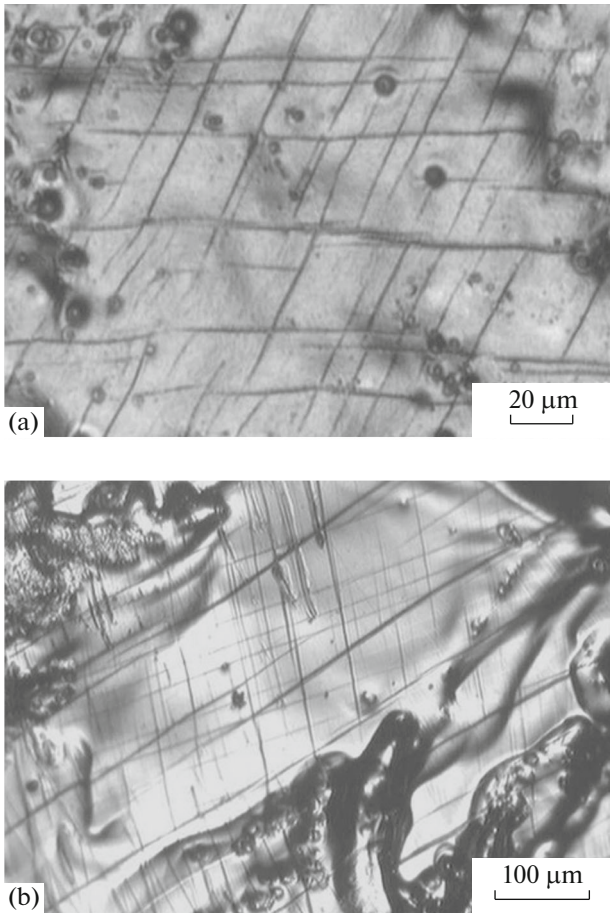

Fig. 9. OM image of the microstructure for the surface areas of the Cu–10% Ga alloy after the action of deuterium plasma and deuterium ions in the PF unit (Experiment 2).

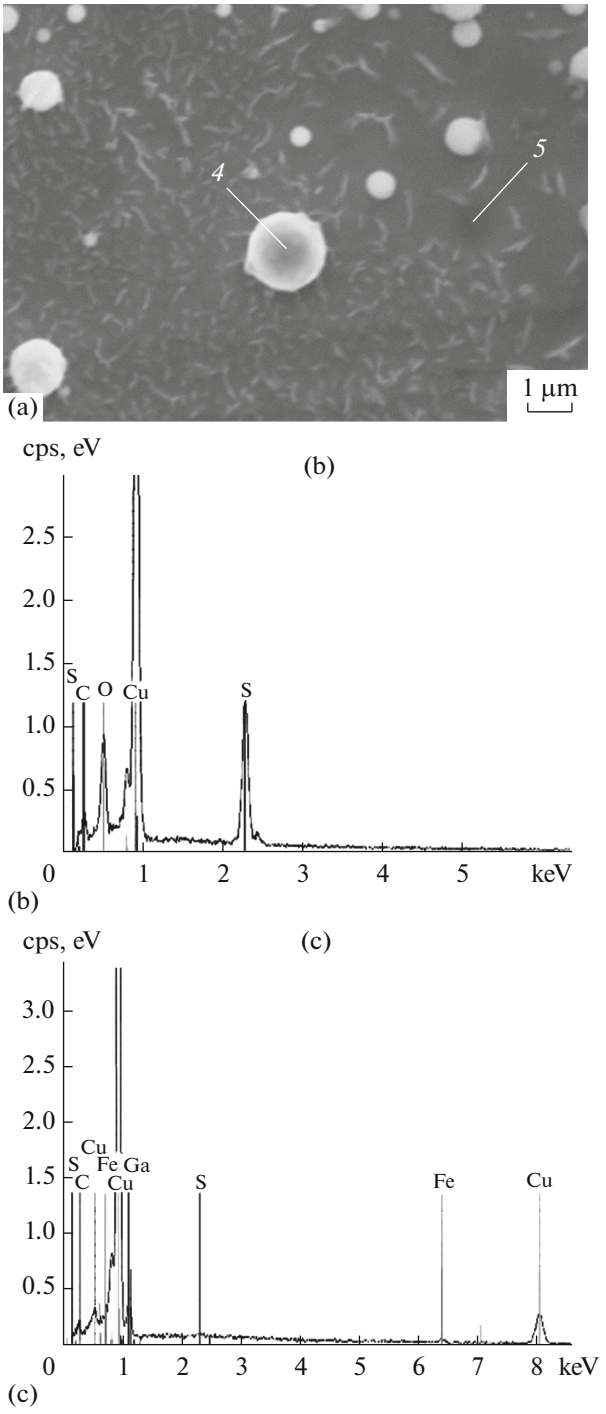

Fig. 10. SEM image of the microstructure (a) and X-ray spectra (b, c) registered for a metal droplet and the surface of the Cu–10% Ga alloy (points *4* and *5* in Fig. 10a) after the action of deuterium plasma and deuterium ions in the PF unit (Experiment 2).

It should be noted that, in addition to the mentioned mechanism of shock-wave action, the material of the target located in the cathode part of the PF chamber is affected by the "gas" SW_g that is created by the working gas plasma (cumulative jet) expanding from the zone of maximum compression (pinch) with each pulse discharge [7].

Since the targets in the PF installations are sufficiently far from the pinch, the conversion of the thermal energy of the pinch into the energy of the directed motion of ions in the plasma incident on the target, as a rule, is completed. In this case, plasma energy flux density $q = nv\frac{mv^2}{2}$, where m is the ion mass, n is the ion concentration, v is the plasma spread velocity.

Since the flux of the pulse, which determines the plasma pressure, can be represented as $P_g = nv \cdot mv$, one can obtain such a simple relation as $P_g = \frac{2q}{v}$. The plasma spread velocity in the PF can be estimated from the condition for the conversion of the thermal energy of the pinch plasma into the energy of directed ion motion as follows:

$$v \approx \left[\frac{3(Z+1)T}{m}\right]^{1/2} \approx (3\text{–}5)\times 10^5 \ \text{m/s},$$

where the deuterium charge $Z = 1$, m is the mass of deuterium, and pinch temperature $T \sim 0.5–1$ keV. Hence, for $q = 10^{10}$ W/cm^2, the required pressure is $P_g \sim 0.5–1$ GPa. A similar estimate for the pressure of the fast ion beam at $q_i = 2 \times 10^{11}$ W/cm^2 and $v = 3 \times 10^6$ m/s gives the value of $P_i = 1.3$ GPa.

The obtained estimates show that the shock-wave loads on the material of the Cu–10% Ga alloy developing under the considered severe irradiation mode, originating both from the action of the cumulative plasma jet ("gas" SW_g) and, especially, from the SW occurring in the bulk of the alloy owing to the effect of the fast ion flux, exceed the critical value of shear stress inherent in copper-based alloys $\sigma_{cr} = 0.4–1.2$ MPa by several orders of magnitude [14].

It is obvious that the action of these pulsed loads is capable of initiating a high-rate plastic deformation process in the material. In this case, the effect of gas shock wave SW_g should precede the radiation-thermal energy flux that falls then to the target in the same pulsed discharge. In addition, the action of such a shock wave can also lead to the revealed destruction of bubbles (Fig. 8b) appearing on the SL surface at the moment of the preceding pulsed action of energy fluxes.

Thus, the block structure formed in the SL of the Cu–10% Ga alloy under a severe irradiation mode (Fig. 9) is the result of plastic deformation of the material caused by three types of loads at each pulsed discharge. First, pulsed shock-wave mechanical loads occur in the gas medium (SW_g and in the bulk of the target sample (SW), and then, at the stage of solidification of the liquid phase and SL cooling, the influence of thermal stresses is observed. The combined effect of these loads of shock-wave and thermal origin exerted on the alloy leads to a nonequilibrium plastic deformation process in the irradiated SL.

At the initial shock-wave stage of irradiation, this process is characterized by a pulsed high-speed development, whereas at the final stage it is determined by the rate of temperature decrease in the heated SL depending on the heat removal conditions. It seems that at different stages the mechanisms of plastic deformation can be different, including twinning and sliding in the closest packing planes {111} typical of materials with the fcc lattice.

CONCLUSIONS

Using the Plasma Focus unit, we have studied the damageability and deformation effects in the surface layers of copper and Cu–10% Ga alloy after irradiation of each of the materials in the following two modes. In one case, the samples were irradiated with pulsed deuterium plasma at a power density of $q_{pl} = 10^7$ W/cm^2 and pulse duration $\tau_{pl} = 100$ ns, whereas in the other case the samples were irradiated by means of a joint action of pulsed fluxes of fast deuterium ions at $q_i = 10^9–10^{11}$ W/cm^2 and at $\tau_i = 50$ ns and dense deuterium plasma at $q_{pl} = 10^8–10^9$ W/cm^2 and at $\tau_{pl} = 100$ ns.

It has been found that, in a less severe irradiation mode (with the use of only plasma flux), the damage level of both materials is close to each other: in the fused surface layer, there are craters, micropores, and an undulating surface that is smoother for the copper-gallium alloy. It has been found that plastic deformation occurred in the SL of this alloy under the action of thermal stresses at the stage of its cooling, as a result of which a block microstructure was formed on the surface after the irradiation.

It is shown that the damageability level exhibits an increase for both materials in a severe irradiation mode (under the combined action of the pulsed fluxes of deuterium ions and deuterium plasma). This is accompanied by the SL erosion and by a possible deposition of elements evaporated from the materials of the working chamber onto the irradiated surface. The most significant damage is observed in the SL of the Cu–10% Ga alloy affected not only by powerful fluxes of ions and plasma but also by shock waves. On the undulating surface of the alloy after irradiation in the considered mode, in addition to micropores and craters, there are microparticles and separate elements composing the functional materials of the PF chamber, as well as bubbles, including those with destroyed dome-like lids.

It has been revealed that a more severe irradiation mode for the materials being compared leads to plastic deformations in the SL. In the case of pure copper at $q = 10^8–10^9$ W/cm^2, the plastic deformations are observed only in separate local zones of the SL, whereas in the case of Cu–10% Ga alloy at $q = 10^{10}–10^{11}$ W/cm^2, this process is observed within the entire irradiated SL. In this case, the mentioned process is observed at each pulsed discharge both under the influence of shock-wave mechanical loads acting on the material at the initial stage of pulsed irradiation and under the influence of thermal stresses occurring at the final stage of the radiation-thermal action.

At different stages of the considered action of energy fluxes on the alloy, the mechanisms of plastic deformation in the SL could be different, including twinning and sliding along closest packing planes {111}, typical of materials with the fcc lattice. However, this issue requires further independent studies.

The method used in this work for the treatment of copper and copper–gallium alloy by a plasma beam impact generated in the Plasma Focus unit within a nanosecond range of pulse duration seems promising for studying high-speed deformation processes occurring in the surface layers of plastic materials under irradiation with powerful pulsed energy fluxes in combination with shock-wave loads.

FUNDING

The work was financially supported according to the State Assignment no. 075-00947-20-00

REFERENCES

1. Shorokhov, E.V., Zhgilev, I.N., Khomskaya, I.V., Brodova, I.G., Zel'dovich, V.I., Gunderov, D.V., Frolova, N.Yu., Gurov, A.A., Oglezneva, N.P., Shirinkina, I.G., Kheifets, A.E., and Astaf'ev, V.V., High-speed deformation of metallic materials using channel angular pressing for producing an ultrafine-grained structure, *Russ. Metall.* (Engl. Transl.), 2010, vol. 2010, no. 4, pp. 323–327.
2. Kovivchak, V.S., Panova, T.V., Blinov, V.I., and Burlakov, R.B., Surface morphology of copper alloys after high power ion beam treatment, *Poverkhn.: Rentgenovskie, Sinkhrotronnye Neitr. Issled.*, 2006, no. 4, pp. 69–71.
3. Zhidkov, M.V., Ligachev, A.E., Kolobov, Yu.R., Potemkin, G.V., and Remnev, G.E., Effect of high-power ion beams on the surface topography and structure of submicrocrystalline titanium alloy subsurface layers, *Russ. J. Non-Ferrous Met.*, 2019, vol. 60, no. 5, pp. 590–597. https://doi.org/10.17073/1997-308X-2018-4-82-91
4. Zhikharev, A.V., Bayankin, V.Ya., Klimova, I.N., Bystrov, S.G., Drozdov, A.Yu., and Kharanzhevskii, E.V., Effect of a focused pulsed laser radiation on the change in the composition and microhardness of surface layers in the $(Cu_{50}Ni_{50})$ + C system, *Phys. Solid State*, 2015, vol. 57, no. 5, vol. 845–855. https://doi.org/10.1134/S1063783415050364
5. Khomskaya, I.V., Zel'dovich, V.I., Frolova, N.Yu., and Kheifets, A.E., Electron microscope study of deformation effects and phase transformations in copper alloys under shock wave loading, *Bull. Russ. Acad. Sci.: Phys.*, 2010, vol. 74, no. 11, pp. 1546–1550.
6. Maslyaev, S.A., Pimenov, V.N., Gribkov, V.A., and Demin, A.S., Damage of chrome-manganese steels by pulsed fluxes of ions and dense plasma under their separate action on the material in the plasma focus setup, *Inorg. Mater.: Appl. Res.*, 2011, vol. 2, no. 5, pp. 445–451.
7. Gribkov, V.A., Demin, A.S., Demina, E.V., Dubrovsky, A.V., Karpinski, L., Maslyaev, S.A., Pimenov, V.N., Padukh, M., and Sholz, M., Physical processes of the interaction of ion and plasma streams with a target surface in a dense plasma focus device, *Plasma Phys. Rep.*, 2012, vol. 38, no. 13, pp. 1082–1089.
8. Gribkov, V.A., Latyshev, S.V., Maslyaev, S.A., and Pimenov, V.N., Numerical simulation of the pulsed energy flow interaction with material in the Plasma Focus device, *Fiz. Khim. Obrab. Mater.*, 2011, no. 6, pp. 16–22.
9. Maslyaev, S.A. Thermal effects during the pulsed irradiation of materials in a Plasma Focus plant, *Perspekt. Mater.*, 2007, no. 5, pp. 47–55.
10. Latyshev, S.A., Gribkov, V.A., Maslyaev, S.A., Pimenov, V.N., Paduch, M., and Zielinska, E., Generation of shock waves in materials science experiments with dense plasma focus device, *Inorg. Mater.: Appl. Res.*, 2015, vol. 6, no. 2, pp. 91–95.
11. Bondarenko, G.G., *Radiatsionnaya fizika, struktura i prochnost' tverdykh tel* (Radiation Physics, Structure, and Strength of Solids), Moscow: Laboratoriya Znanii, 2016.
12. Demina, E.V., Ivanov, L.I., Maslyaev, S.A., Pimenov, V.N., Sasinovskaya, I.P., Gribkov, V.A., and Dubrovskii, A.V., Surface modification of steel pipes by pulsed ion and high-temperature plasma fluxes, *Perspekt. Mater.*, 2008, no. 5, pp. 41–48.
13. Lyakishev, N.P., *Diagrammy sostoyanii dvoinykh metallicheskikh sistem: Spravochnik* (State Diagram of Double Metal Systems: Handbook), Moscow: Mashinostroenie, 1996, vol. 1.
14. Nikolaeva, E.A., *Sdvigovye mekhanizmy plasticheskoi deformatsii monokristallov. Uchebnoe posobie* (Shear Mechanisms of Plastic Deformation of Single Crystals: Manual), Perm: Perm. Gos. Tekh. Univ., 2011. http://lab4.icmm.ru/wp-content/uploads/2012/05/nikolaeva2.pdf.
15. Hirai, T., Pintsuk, G., Linke, J., and Batilliot, M., Cracking failure study of ITER-reference tungsten grade under single pulse thermal shock loads at elevated temperatures, *J. Nucl. Mater.*, 2009, vols. 390–391, pp. 751–755.
16. Garkusha, I.E., Burdakov, A.V., Ivanov, I.A., Kruglyakov, E.P., et al., Plasma surface interaction during ITER transient events simulation with QSPA Kh-50 and Gold-3 facilities, *Probl. At. Sci. Technol., Ser.: Plasma Phys.*, 2008, vol. 14, no. 6, pp. 58–60.
17. Borovitskaya, I.V., Pimenov, V.N., Gribkov, V.A., Padukh, M., Bondarenko, G.G., Gaidar, A.I., Paramonova, V.V., and Morozov, E.V., Structural changes in the vanadium sample surface induced by pulsed high-temperature deuterium plasma and deuterium ion fluxes, *Russ. Metall.* (Engl. Transl.), 2017, vol. 2017, no. 11, pp. 928–935.
18. Voronin, A.V., Semenov, B.N., and Sud'enkov, Yu.V., Fracture mechanism of tungsten as a result of heat loading affected by plasma jet, *Vestn. S.-Peterb. Gos. Univ., Matem.*, 2015, vol. 2 (60), no. 1, pp. 106–111.
19. Demin, A.S., Maslyaev, S.A., Pimenov, V.N., Gribkov, V.A., Demina, E.V., Latyshev, S.V., Lyakhovickii, M.M., Sasinovskaya, I.P., Bondarenko, G.G., Gaydar, A.I., and Padukh, M.,, *Fiz. Khim. Obrab. Mater.*, 2017, no. 6, pp. 5–17.
20. Paju, J., Väli, B., Laas, T., Shirokova, V., Laas, K., Paduch, M., Gribkov, V.A., Demina, E.V., Prusakova, M.D., Pimenov, V.N., Makhlaj, V.A., and Antonov, M., Generation and development of damages in double forged tungsten in different combined regimes of irradiation with extreme heat loads, *J. Nucl. Mater.*, 2017, vol. 495, pp. 91–102.
21. Budaev, V.P., Martynenko, Yu.V., Karpov, A.V., Belova, N.E., Zhitlukhin, A.M., Klimov, N.S., et al., Tungsten recrystallization and cracking under ITER relevant heat loads, *Vopr. At. Nauki Tekh., Ser.: Termoyad. Sint.*, 2015, vol. 463, pp. 237–240.
22. Javadi, S., Ouyang, B., Zhang, Z., Ghoranneviss, M., Salar Elahi, A., and Rawat, R.S., Effects of fusion relevant transient energetic radiation, plasma and thermal load on PLANSEE double forged tungsten samples in a low energy plasma focus device, *Appl. Surf. Sci.*, 2018, vol. 443, pp. 311–320.
23. Herashchenko, S.S., Makhlaj, V.A., Aksenov, N.N., Garkusha, I.E., Byrka, O.V., Kulik, N.V., Chebotarev, V.V., and Staltsov, V.V., Erosion of the combined three-dimensional tungsten target under the impacts of QSPA Kh-50 powerful plasma streams, *Ukr. J. Phys.*, 2016, vol. 61, no. 7, pp. 578–582.

Translated by O. Polyakov